Journal of Materials Chemistry A

Accepted Manuscript

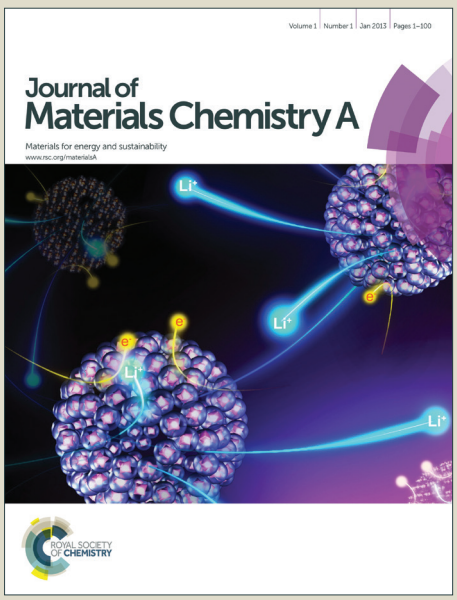

ROYAL SOCIETY OF CHEMISTRY

www.rsc.org/materialsA

Cite this: DOI: 10.1039/c0xx00000x

www.rsc.org/xxxxxx

ARTICLE TYPE

Effective passivation of a high-voltage positive electrode by 5-hydroxy-1H-indazole additive

Yoon-Sok Kang,[a] Taeho Yoon,[c] Junyoung Mun,[a, d] Min Sik Park,[a] In-Yong Song,[b] Anass Benayad,[b] Seung M. Oh,*[c]

Received (in XXX, XXX) Xth XXXXXXXXX 20XX, Accepted Xth XXXXXXXXX 20XX
DOI: 10.1039/b000000x

5-hydroxy-1H-indazole (HI) is investigated as an effective film-forming additive for an over-lithiated layered oxide (OLO) positive electrode. The protective film that is generated by oxidative decomposition of the additive (HI) prior to the carbonate electrolyte is thin and less resistive. As a result, a full cell comprised of OLO/graphite in HI-added electrolyte gives a better cycling performance.

.

Introduction

Ever since SONY first commercialized lithium-ion batteries (LIBs) in 1992, the market of LIBs has been steadily expanding. LIBs have typically been used to power small electronic devices such as mobile phones and laptop computers [1]. More recently, LIBs have been drawing more attention for their potential use in larger power sources, which include electric vehicles and energy storage systems, because of fluctuating oil prices and resources as well as the increasing awareness of global environmental issues [2–3]. The current performance level of LIBs, however, does not meet the standards for new applications with regards to energy density, cycle life, and safety. When the designed application requires a large consumption of electrical energy, e.g., in an electric vehicle, the deficient energy density of LIBs presents one of the biggest challenges owing to the restriction of space and the poor energy efficiency that derives from the vehicle's mass.

LIBs produce and store electrochemical energy through lithium ion/electron transfer. When LIBs are assembled, the positive electrode contains lithium compounds such as $LiCoO_2$, $LiMn_2O_4$, and $LiFePO_4$. Accordingly, the energy density of LIBs is determined by the amount of lithium ions in positive electrodes. Notable electrode materials known as lithium-excess layered oxides (also known as over-lithiated layered oxides, OLO), $Li_{1+x}Mn_yCo_zNi_aO_2$, have a higher working voltage (up to 4.9 V *vs.* Li/Li^+) and larger specific capacity than those of $LiCoO_2$ and $LiMn_2O_4$ [4-12]. With OLOs, the charging voltage must be beyond 4.5 V to use effectively the lithium ions in the transition metal layer. Although the high working potential is beneficial for high energy density, it brings about oxidative decomposition of electrolytes due to their narrow electrochemical stability window [13-14]. Even if the calculated oxidation potential of carbonate solvents are above 6 V (*vs.* Li/Li^+), they are oxidized at lower potentials due to the catalytic effect of the transition metal ions in positive electrodes [15].

A surface passivation layer is usually introduced to address the issue of electrolyte decomposition. This surface film-based electrochemical defense has been vigorously studied on negative electrodes and is called solid electrolyte interface or interphase (SEI) [16-23]. Aiming to form an artificial SEI layer on negative electrode surface, additives that are decomposed prior to the electrochemical breakdown of electrolyte have been investigated. Much efforts have been devoted to the formation of a stable SEI on negative electrodes using additives including vinylene carbonate (VC), fluoroethylene carbonate (FEC), lithium bis(oxalate) borate (LiBOB), lithium difluoro(oxalate) borate (LiFOB), and succinic anhydride (SA) [24-39]. Film-forming additives on positive electrodes, however, have rarely been investigated beyond the concept of overcharge protection [40-47].

The surface film derived from either electrolytes or additives must be able to pass lithium ions but not electrons, and its thickness should be controlled to successfully pass lithium ions without high resistance. In this work, 5-hydroxy-1H-indazole (HI hereafter) has been investigated as a candidate for an additive. Its oxidation potential was calculated by using density functional theory (DFT) and was compared with those of the carbonate solvents to confirm its feasibility for film formation. The electrochemical characteristics of the HI-derived passivation film were examined at an elevated temperature (45°C) for an accelerated cycle test.

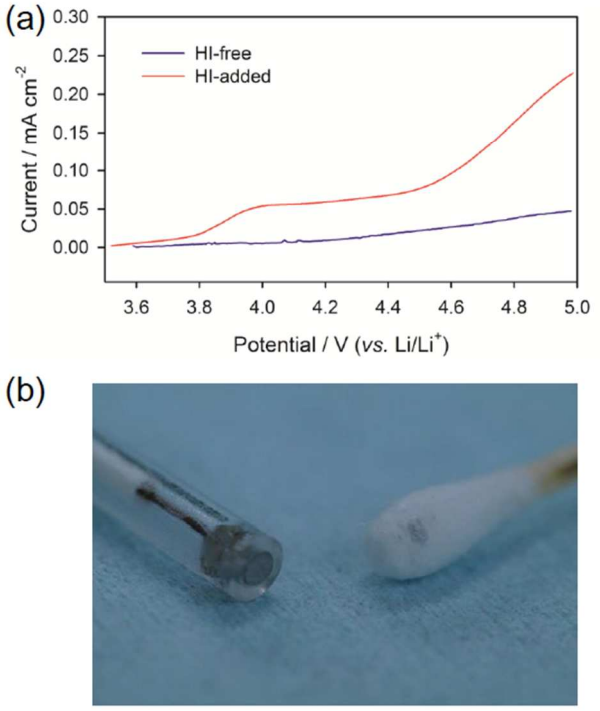

Figure 1. (a) Linear sweep voltammograms traced in two electrolytes on a Pt working electrode and (b) image of a Pt electrode and the cotton swab that was used to wipe it after LSV with HI-added electrolyte.

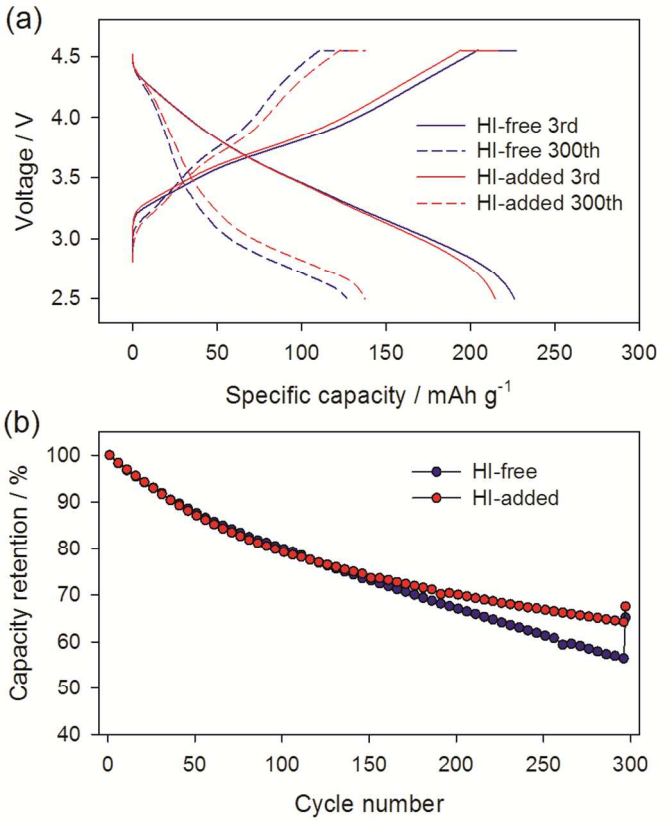

Figure 2. Charge-discharge performance of OLO/graphite full cell in two electrolytes, which were HI-free (red) and HI-added (blue). 45 °C (a) capacity-voltage plots for the 3rd and the 300th cycles (b) discharge capacity retention observed.

Experimental

For the ab-initio calculations of the oxidation and reduction potentials, the optimized geometry of the target molecules was obtained at the B3 LYP/6-311+G (d,p) level as implemented in Gaussian 03 [48]. The polarized continuum model was also employed to describe the bulk solvent effect [49]. The oxidation/reduction (redox) potential was calculated based on the following redox reaction:

$$HI\ (solution) \rightarrow HI^{+}\ (solution) + e^{-}\ (gas)$$

$$HI\ (solution) + e^{-}\ (gas) \rightarrow HI^{-}\ (solution)$$

Linear sweep voltammograms (LSV) were taken in a three-electrode cell, in which a Pt disk was used as the working electrode and lithium foils functioned as the counter and reference electrode. The used electrolyte was 1.3 *M* $LiPF_6$ dissolved in fluoroethylene carbonate (FEC)/dimethyl carbonate (DMC) (v/v, 3:7), which hereafter will be referred to as HI-free electrolyte. Another electrolyte solution was prepared by adding 5-hydroxy-1H-indazole (HI) into the HI-free electrolyte at a concentration of 0.1 wt% (HI-added electrolyte).

The Li-excess transition metal oxide (OLO) used in the present study was synthesized by a co-precipitation method. The transition metal precursors of nickel sulfate ($NiSO_4$•$6H_2O$), cobalt sulfate ($CoSO_4$•$7H_2O$), and manganese sulfate ($MnSO_4$•H_2O) were dissolved in distilled water. The transition metal solution was slowly added drop-wise to the aqueous NaOH solution. The precipitated powder obtained by washing, filtration, and drying for 24 h at 120°C was mixed with Li_2CO_3 and then fired at 900°C for 10 h in air. The composite positive electrode was prepared from an OLO powder ($Li_{1.17}Mn_{0.50}Co_{0.17}Ni_{0.17}O_2$, 8.5 mg cm^{-2}), Denka black, and poly(vinylidene fluoride) (PVdF, Solef) at a 90:5:5 weight ratio on aluminum foil; the negative electrode was prepared from a graphite powder and a CMC-SBR binder (carboxymethyl cellulose; styrene-butadiene rubber) on a copper foil. A polyethylene film coated with Al_2O_3 particles (Teijin) was used as a separator. The capacity ratio between the negative and positive electrode was 1.15, and the full-cell capacity was 3 mA·h.

Both types of cells were initially cycled twice at 25°C over a 2.5–4.55 V range at a current of 0.1 C to complete the formation process. Galvanostatic charge/discharge cycling was conducted with the full cells at 45°C in the same potential range and at 250 mA·g^{-1} (1C). For complete charging, an additional constant-voltage step was added at 4.55 V. Impedance was measured using a Solartron 1287 potentiostat/galvanostat (Solartron Analytical, U.K.). The frequency range and voltage amplitude were set to 100 MHz to 0.1 Hz and 10 mV, respectively. For the scanning electron microscopic (SEM, Hitachi S4500) and X-ray photoelectron spectroscopic (XPS, Sigma probe, Thermo, U.K.) analyses, the cycled cells were dismantled in an argon-filled

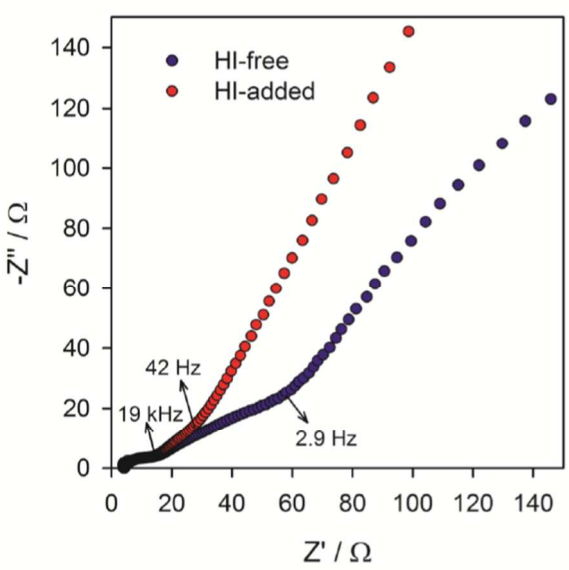

Figure 3. AC impedance spectra obtained after 300 cycles at 45°C.

glove box, and the collected electrodes were rinsed with DMC. The binding energy was calibrated using the C1s peak at 285 eV obtained from the C–C bond.

Results and Discussion

The calculated oxidation potentials (E_{ox}) for HI, DMC, and FEC are 4.13, 6.78, and 7.51 V (*vs*. Li/Li^+), respectively. HI shows a lower E_{ox} than those of the carbonate solvents, thus it is expected to decompose on the positive electrode prior to the carbonate solvents. This feature is observed on the LSVs shown in Fig 1a. The oxidation current of HI-free electrolyte shows a monotonous increase. When 0.1 wt% of HI is added, however, an oxidation peak appears at 4 V, which confirms that HI is oxidized earlier than the carbonate solvents. After LSV in the presence of the HI-added electrolyte, the Pt electrode was visually coated with a dark, sticky material that could be removed with a cotton swab as shown in Fig. 1b. In the case of the HI-free electrolyte, however, nothing was observed to be wiped off with a cotton swab. These results demonstrate a possible film formation on the working electrode by HI.

Fig. 2a shows the charge-discharge voltage profiles of the full cell obtained in two electrolytes. In the 3rd cycle, the discharge capacity of the HI-added cell is slightly lower than that for the HI-free cell. After 300 cycles, however, the HI-added cell exhibits larger discharge capacity than that of the HI-free cell. Additionally, the HI-added cell exhibits smaller cell polarization in the 300th cycle, which is also confirmed in the AC impedance data shown in Fig. 3. The impedance of HI-added cell is significantly smaller than that of the HI-free cell. The cycling results of the OLO/graphite cells that were cycled within 2.5–4.55 V range at 45°C in both electrolytes are shown in Fig. 2b. For the cells cycled in the HI-added electrolyte, a much better retention of the capacity is observed.

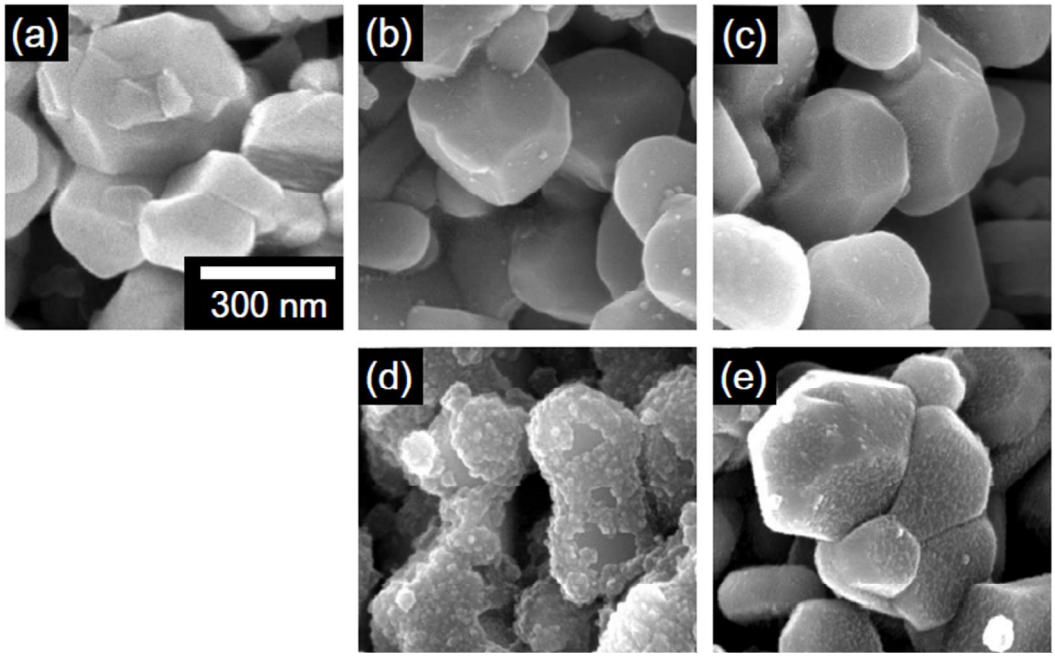

Figure 4. The SEM images of OLO composite electrode surface: (a) pristine OLO, (b) cycled twice in the HI-free electrolyte, (c) cycled twice in the HI-added electrolyte (d) cycled 300 times in the HI-free electrolyte, and (e) cycled 300 times in the HI-added electrolyte.

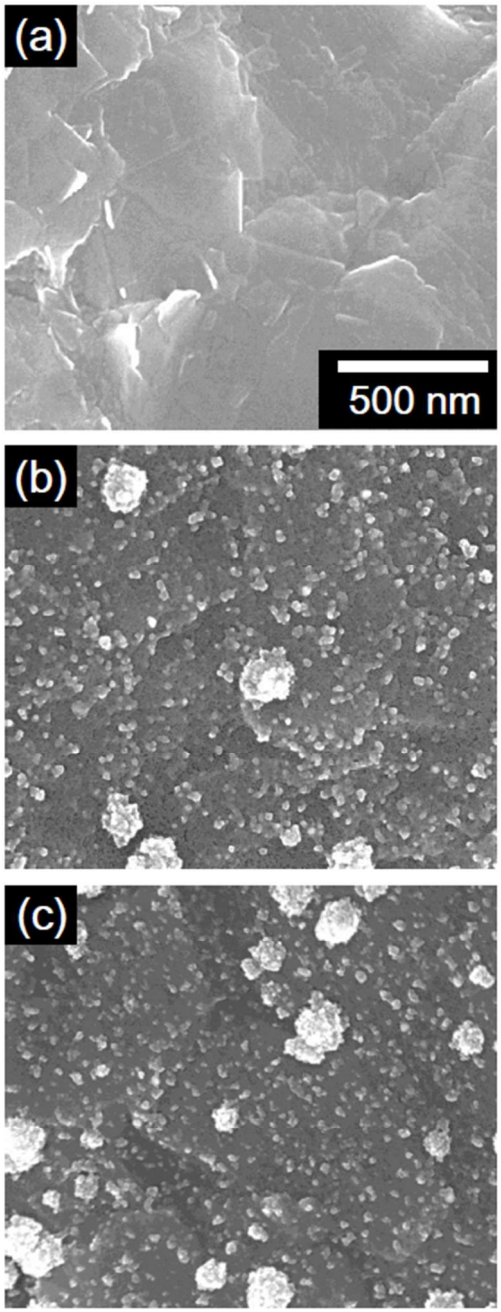

Figure 5. The SEM images of graphite composite electrode surface: (a) pristine graphite, (b) cycled 300 times in the HI-free electrolyte, and (c) cycled 300 times in the HI-added electrolyte.

To address the difference in cell polarization and capacity retention for two cells, *ex-situ* HRSEM analysis was performed on the OLO electrode surfaces. Fig. 4a displays the SEM image taken from the pristine OLO electrode, in which the sharp edges of OLO particles can be clearly observed. Fig. 4b and 4c illustrate that thin surface films deposit from both electrolytes in the earlier cycles. After prolonged cycling, the formation of a thick surface film is noticed on the OLO electrode cycled in the HI-free electrolyte (Fig. 4d). Note that surface films are usually resistive ion migration, such that a deposition of thick surface films leads

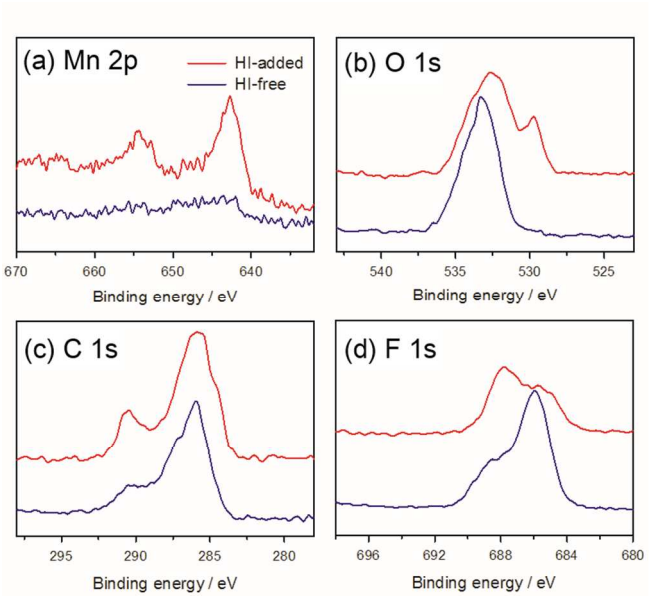

Figure 6. The XPS spectra obtained from the OLO electrodes that were cycled 300 times in two electrolytes.

to an enlargement in cell polarization. In contrast, the micrograph of the positive electrode cycled 300 times in the HI-added cell portrays a much thinner surface film (Fig. 4e). Hence, a less significant cell polarization is assumed, which is in accordance with the results shown in Fig. 2a and Fig. 3. The detailed discussion on this will be advanced in the later section. Surface films are also formed on the graphite negative electrode as shown in Fig. 5. Unlike the OLO positive electrode, however, the films on the graphite surface exhibits little difference between the electrolytes as shown in Fig. 5b and 5c. It is thus very likely that the HI additive effectively passivates only the positive electrode, which correlates with the expectations deduced from the redox potential calculations by Gaussian 03. It should be noted that the reduction potential of HI is calculated to be 0.26 V, which is far lower than those of the cyclic carbonates. In that case, the preformed surface film on graphite by reduction of carbonate solvents prevents further decomposition of HI.

Fig. 6 presents the XPS core peaks of Mn 2p, O 1s, C 1s, and F 1s registered at the OLO electrode surfaces after 300 cycles. The peak intensity for Mn 2p photoelectrons is weaker for the OLO electrode that is cycled in the HI-free electrolyte, indicative of a deposition of thicker surface film on it. This feature is further confirmed on the O 1s and C 1s spectra. As shown in Fig. 6b, the O 1s photoelectrons emitted from the oxide ions (O^{2-}) in the OLO lattice (529.8 eV) is negligible for this electrode. The C1s photoelectrons coming from the C-F carbons in PVdF (290.4 eV) are also weak in their intensity (Fig. 6c). The very weak or negligible peak intensity for Mn 2p and O 1s photoelectrons from the OLO lattice, and C 1s photoelectrons from PVdF clearly indicates that the surface of composite electrode is covered by a thick surface film. This feature is contrasted by the OLO electrode cycled in the HI-added electrolyte. The peak intensity for the above-mentioned photoelectrons is much stronger than that observed in the HI-free cell, indicating that the composite electrode surface is not buried by thick film. Meanwhile, the O 1s

spectra at 530-537 eV and the C 1s spectra at 283-289 eV are comparable for two samples. This implies that the C or O species that are derived from the electrolytes are similar for two samples. The difference in chemical composition of films can be found in the F 1s spectra (Fig. 6d). The F1s peak at the higher binding energies (around 687.6 eV) can be assigned to $LiPF_6$ or CF_2 in PVdF, whereas the peak at 685 eV is assigned to LiF. Prominently, the population of LiF is much larger in the OLO surface that is cycled without the additive. LiF is known to be much more resistive than surface films comprised of carbonates [17-18,36,50-51]. Therefore, when the electrode underwent prolonged cycling without the additive, it had more sluggish kinetics due to the formation of thick and resistive surface films. This is evidenced by the larger diameter of the high frequency semicircle in the Nyquist plot of the cycled electrode. The XPS data of the graphite electrodes after cycling are shown in Supplementary Figure 1, and many of the same XPS peaks were observed. These results corroborate that HI selectively affects the passivation of the positive electrode in accordance with SEM.

Conclusions

5-hydroxy-1H-indazole (HI) is electrochemically oxidized prior to the carbonate solvents to form a passivating film on OLO surface. Due to this passivating film, the cell polarization is slightly larger in the earlier cycles as compared to that observed in the HI-free electrolyte. However, the passivating ability of HI derived film is excellent, such that additional electrolyte decomposition and film growth are not significant. As a result, the increment of cell polarization is not severe to yield better cycling performance. In contrast, the passivating ability of the surface film derived from the HI-free electrolyte is poorer to allow a continued growth of surface film, in which the population of highly resistive LiF is predominant. HI is not effective for the passivation of graphite negative electrode since its reduction potential is lower than that for the carbonate solvents.

Notes and references

[a] *Energy Material Lab and* [b]*Analytical Engineering Group, SAIT, Samsung Electronics Co. Ltd., Gyeonggi-do 443-803, Korea*
[c] *Department of Chemical and Biological Engineering, Institute for Chemical Processes, Seoul National University, Seoul 151-744, Korea*
[d] *Department of Energy and Chemical Engineering, Incheon National University, 12-1, Songdo-dong, Yeonsu-gu, Incheon 406-840, Korea*
**Corresponding author: Fax: +82 2 872 5755, Tel.: +82 2 880 7074; E-mail address: seungoh@snu.ac.kr (S. M. Oh).*
S. M. Oh acknowledges the financial support from National Research Foundation of Korea funded by the MEST (NRF-2010-C1AAA001-2010-0029065).

† Electronic Supplementary Information (ESI) available: [details of any supplementary information available should be included here]. See DOI: 10.1039/b000000x/

1 B. Scrosati, J. Garche, *J. Power Sources*, 2010, **195,** 2419
2 M. Armand, J.- M. Tarascon, *Nature*, 2008, **451**, 652
3 J. Tollefson, *Nature*, 2008, **456**, 436
4 M. Hu, X. Pang, Z. Zhou, *J. Power Sources*, 2013, **237**, 229
5 T. Yoon, S. Park, J. Mun, J. Ryu, W. Choi, Y. Kang, J. Park, S. Oh, *J. Power Sources*, 2012, **215**, 312
6 M. Thackeray, S. Kang, C. S. Johnson, J. T. Vaughey, R. Benedek, S. A. Hackney, *J. Mater. Chem*., 2007, **17**,3112
7 J. B. Goodenough, Y. Kim, *Chem. Mater*., 2010, **22**, 587
8 N. Yabuuchi, K. Yoshii, S. T. Myung, I. Nakai, S. Komaba, *J. Am. Chem. Soc*., 2011, **133**, 4404
9 J.-H Park, J. Lim, J. Yoon, K.-S. Park, J. Gim, J. Song, H. Park, D. Im, M. Park, D. Ahn, Y. Paik, J. Kim, *Dalton Trans*., 2012, **41**, 3053
10 S.-H. Yu, T. Yoon, J. Mun, S. Park, Y.-S. Kang, J.-H. Park, S.M. Oh, Y.-E. Sung, *J. Mater. Chem. A*, 2013, **1**, 2833
11 Y. Li, M. Bettge, B. Polzin, Y. Zhu, M. Balasubramanian, D. P. Abraham, *J. Electrochem. Soc*., 2013, **160**, A3006
12 Y. Zhu, Y. Li, M. Bettge, D. P. Abraham, *J. Electrochem. Soc*., 2012, **159**, A2109
13 L. Yang, B. Ravdel, B. L. Lucht, *Electrochem. Solid-State Lett*., 2010, **13**, A95
14 S. K. Martha, J. Nanda, G. M. Veith, N. J. Dudney, *J. Power Sources*, 2012, **216**, 179
15 K. Xu, S.P. Ding, T.R. Jow, *J. Electrochem. Soc*. 1999, **146**, 4172
16 E. Peled, D. Golodnisky, G. Ardel, *J. Electrochem. Soc*., 1997, **144**, L208
17 D. Aurbach, B. Markovsky, A. Rodkin, M. Cojocaru, E. Levi, H.-J. Kim, *Electrochim. Acta*, 2002, **47**, 1899
18 B. Markovsky, A. Rodkin, Y. S. Cohen, O. Palchik, E. Levi, D. Aurbach, H.-J. Kim, M. Schmidt, *J. Power Sources*, 2003, **119-121**, 504
19 K. Xu, *Chem. Rev*., 2004, **104**, 4303
20 S. Zhang, *J. Power Sources*, 2006, **162**, 1379
21 P. Verma, P. Maire, P. Novak, *Electrochim. Acta*, 2010, **55**, 6332
22 K. Xu, A. von Cresce, *J. Mater. Chem*., 2011, **21**, 9849
23 H. Buqa, P. Golob, M. Winter, J. O. Besenhard, *J. Power Sources*, 2001, **97-98**, 122
24 S.-K. Jeong, M. Inaba, R. Mogi, Y. Iriyama, T. Abe. Z. Ogumi, *Lamgmuir*, 2001, **17**, 8281
25 D. Aurbach, K. Gamolsky, B. Markovsky, Y. Gofer, M. Schmidt, U. Heiter, *Electrochim. Acta*, 2002, **47**, 1423
26 K. Xu, S. Zhang, T.R. Jow, *Electrochem. Solid State Lett*., 2005, **8**, A365
27 N.-S. Choi, K.H. Yew, K.Y. Lee, M. Sung, H. Kim, S.-S. Kim, *J. Power Sources*, 2006, **161**. 1254
28 L. Chen, K. Wang, X. Xie, J. Xie, *J. Power Sources*, 2007, **174**, 538
29 N.-S. Choi, K.H. Yew, H. Kim, S.-S. Kim, W.-U. Choi, *J. Power Sources*, 2007, **172**, 404
30 J. Liu, Z. Chen, S. Busking, K. Amine, *Electrochem. Comn.,* 2007, **9**, 475
31 H. Lee, S. Choi, S. Choi, H.-J. Kim, Y. Choi, S. Yoon, J.-J. Cho, *Electrochem. Comn.,* 2007, **9**, 801
32 Y. Qin, Z. Chen, W. Lu, K. Amine, *J. Power Sources*, 2010, **195**, 6888
33 G.-B. Han, M.-H. Ryou, K.Y. Cho, Y.M. Lee, J.-K. Park, *J. Power Sources*, 2010, **195**, 3709
34 A. von Cresce, K. Xu, *J. Electrochem. Soc.*, 2011, **158**, A337
35 V. Etacheri, O. Haik, Y. Goffer, G.A. Roberts, I.C. Stefan, R. Fasching, D. Aurbach, *Lamgmuir*, 2012, **28**, 965
36 S. Dalavi, P. Guduru, B. Lucht, *J. Electrochem. Soc*., 2012, **159**, A642
37 Y.-M. Lin, K.C. Kalvetter, P.R. Abel, N.C. Davy, J.L. Snider, A. Heller, C.B. Mullins, *Chem. Comn*, 2012, **48**, 7268
38 K. Ushirogata, K. Sodeyama, Y. Okuno, Y. Tateyama, *J. Am. Chem. Soc.*, 2013, **135**, 11967
39 H. Jung, S.-H. Park, J. Jeon, Y. Choi, S. Yoon, J.-J. Cho, S. Oh, S. Kang, Y.-K. Han, H. Lee, *J. Mater. Chem. A*, 2013, **1**, 11975
40 Y. Watanabe, H. Morimoto, S. Tobishima, *J. Power Sources*, 2006, **154**, 246
41 B. Wang, Q. Xia, P. Zhang, G. C. Li, Y. P. Wu, H. J. Luo, S. Y. Zhao, T. van Ree, *Electrochem. Comm*., 2008, **10**, 727
42 K. Abe, T. Takaya, H. Yoshitake, Y. Ushigoe, M. Yoshio, H. Wang, *Electrochem. Solid-state Lett*., 2004, **7**, A462
43 K. Lee, Y. Sun, J. Noh, K. Song, D. Kim, *Electrochem. Comm*., 2009, **11**, 1900

44 T. Kubota, M. Ihara, S. Katayama, H. Nakai, J. Ichikawa, *J. Power Sources*, 2012, **207**, 141

45 R. Sharabi, E. Markevich, K. Fridman, G. Gershinsky, G. Salitra, D. Aurbach, G. Semrau, M.A. Schmidt, N. Schall, C. Bruenig, *Electrochem. Comm.*, 2013, **28**, 20

46 V. Tarnopolskiy, J. Kalhoff, M. Nadherna, D. Bresser, L. Picard, F. Fabre, M. Rey, S. Passerini, *J. Power Sources*, 2013, **236**, 39

47 Y.-S. Kang, T. Yoon, S. Lee, J. Mun, M. S. Park, J.-H. Park, S.-G. Doo, I.-Y. Song, S. M. Oh, *Electrochem. Comm.*, 2013, **27**, 26

48 M. J. Frisch, G. W. Trucks, H. B. Schlegel, G. E. Scuseria, M. A. Robb, J. R. Cheeseman, J. A. Montgomery Jr., T. Vreven, K..N. Kudin, J. C. Burant, J. M. Millam, S. S.Iyengar, J. Tomasi, V. Barone, B. Mennucci, M. Cossi, G. Scalmani, N. Rega, G. A.Petersson, H. Nakatsuji, M. Hada, M. Ehara, K. Toyota, R. Fukuda, J. Hasegawa, M.Ishida, T. Nakajima, Y. Honda, O. Kitao, H. Nakai, M. Klene, X. Li, J. E. Knox, H. P.Hratchian, J. B. Cross, V. Bakken, C. Adamo, J. Jaramillo, R. Gomperts, R. E. Stratmann, O. Yazyev, A. J. Austin, R. Cammi, C. Pomelli, J. W. Ochterski, P. Y. Ayala, K. Morokuma, G. A. Voth, P. Salvador, J. J. Dannenberg, V. G. Zakrzewski, S. Dapprich, A. D. Daniels, M. C. Strain, O. Farkas, D. K. Malick, A. D. Rabuck, K. Raghavachari, J. B. Foresman, J. V. Ortiz, Q. Cui, A. G. Baboul, S. Clifford, J. Cioslowski, B. B. Stefanov, G. Liu, A. Liashenko, P. Piskorz, I. Komaromi, R. L. Martin, D. J. Fox,T. Keith, M. A. Al-Laham, C. Y. Peng, A. Nanayakkara, M. Challacombe, P. M. W. Gill, B. Johnson, W. Chen, M. W. Wong, C. Gonzalez, J. A. Pople, Gaussian 03.

49 J. Tomasi, B. Mennucci, R. Cammi, *Chem. Rev.*, 2005, **105**, 2999

50 M. Herstedt, M. Stjerndahl, T. Gustafsson, K. Edstrom, *Electrochem. Comn.*, 2003, **5**, 467

51 D. Aurbach, B. Markovsky, G. Salitra, E. Markevich, Y. Talyossef, M. Koltypin, L. Nazar, B. Ellis, D. Kovacheva, *J. Power Source*, 2007, **165**, 491